



Published in final edited form as:

Clin Cancer Res. 2019 July 15; 25(14): 4542–4551. doi:10.1158/1078-0432.CCR-18-3004.

Down-regulation of human DAB2IP Gene Expression in Renal Cell Carcinoma Results in Resistance to Ionizing Radiation

Eun-Jin Yun^{1,2}, Chun-Jung Lin¹, Andrew Dang¹, Elizabeth Hernandez¹, Jiaming Guo³, Wei-Min Chen³, Joyce Allison⁴, Nathan Kim³, Payal Kapur⁵, James Brugarolas⁴, Kaijie Wu⁶, Dalin He⁶, Chih-Ho Lai⁷, Ho Lin⁸, Debabrata Saha³, Seung Tae Baek^{2,*}, Benjamin P.C. Chen^{3,*}, and Jer-Tsong Hsieh^{1,9,*}

¹Department of Urology, University of Texas Southwestern Medical Center, Dallas, TX 75390, USA;

²Division of Integrative Bioscience and Biotechnology, POSTECH, Pohang 37673, Republic of Korea;

³Department of Radiation Oncology, University of Texas Southwestern Medical Center, Dallas, TX 75390;

⁴Department of Internal Medicine and Kidney Cancer Program, Simmons Comprehensive Cancer Center, University of Texas Southwestern Medical Center, Dallas, TX 75390;

⁵Department of Pathology, University of Texas Southwestern Medical Center, Dallas, TX 75390;

⁶Department of Urology, The First Affiliated Hospital, Medical School of Xi'an Jiaotong University, Xi'an 710049, China;

⁷Department of Microbiology and Immunology, Graduate Institute of Biomedical Sciences, College of Medicine, Chang Gung University, Taoyuan, Taiwan;

⁸Department of Life Sciences, National Chung Hsing University, Taichung, Taiwan;

⁹Graduate Institute of Cancer Biology, China Medical University Hospital, Taichung 40447, Taiwan, Republic of China

Abstract

Purpose: Renal cell carcinoma (RCC) is known to be highly radio-resistant but the mechanisms associated with radio-resistance have remained elusive. We found DAB2IP frequently down-regulated in RCC, is associated with radio-resistance. In this study, we investigated the underlying mechanism regulating radio-resistance by DAB2IP and developed appropriate treatment.

Experimental design: Several RCC lines with or without DAB2IP expression were irradiated with ionizing radiation (IR) for determining their radio-sensitivities based on colony formation assay. To investigate the underlying regulatory mechanism of DAB2IP, immunoprecipitation-mass-spectrometry (IP-MS) was performed to identify DAB2IP-interactive proteins. poly (ADP-ribose)

*Contributed as co-corresponding authors: Jer-Tsong Hsieh, Ph.D., jt.hsieh@utsouthwestern.edu; Benjamin P.C. Chen Ph.D., Benjamin.Chen@UTSouthwestern.edu; Seung Tae Baek, Ph.D., sbaek@postech.ac.kr.

All the authors have no conflict of interest.

polymerase-1 (PARP-1) expression and enzymatic activity were determined using quantitative real-time PCR, Western blot and ELISA. *In vivo* ubiquitination assay was employed to test PARP-1 degradation. Furthermore, *in vivo* mice xenograft model as well as patient-derived xenograft (PDX) model was employed to determine the effect of combination therapy to sensitizing tumors to IR.

Results: We notice that DAB2IP-deficient RCC cells acquire IR-resistance. Mechanistically, DAB2IP can form a complex with PARP-1 and E3 ligases that is responsible for degrading PARP-1. Indeed, elevated PARP-1 levels are associated with the IR resistance in RCC cells. Furthermore, PARP-1 inhibitor can enhance the IR response of either RCC xenograft model or PDX models.

Conclusions: In this study, we unveil that loss of DAB2IP resulted in elevated PARP-1 protein is associated with IR-resistance in RCC. These results provide a new targeting strategy to improve the efficacy of radiotherapy of RCC.

Introduction

Ionizing radiation (IR) can be a very effective regimen for targeting localized tumors or areas of invasion after surgical resection (1). Recent advances in external beam radiotherapy (RT) have significantly improved the therapeutic index by combining both imaging-guided precision targeting with the delivery of high doses using three-dimensional fractionation. The major trigger of the cellular response to IR is its destructive impact on genome integrity. Cells can mount a coordinated response to IR by activating a network of interacting signaling pathways, collectively known as the DNA damage response (DDR) (2). There are two main pathways to repair DNA double-strand breaks (DSB): Non-homologous end joining (NHEJ) and homologous recombination (HR) (3,4). In response to DSB formation, it has been shown that phosphorylation of H2AX occurs in the position of Ser139, then many DDR proteins such as RAD50, MDC1, and BRCA-1 attracted to γ H2AX foci (5,6). Subsequently, DNA-binding enzyme poly(ADP-ribose) polymerase 1 (PARP-1) is recruited to modulate the activity of the DNA repair systems (7,8) and has a primary role in the process of poly(ADP-ribosyl)ation, which is responsible for the major poly(ADP-ribosyl)ation activity observed during DDR. PARP-1 binds to the damaged DNA sites and initiates the formation of a poly-ADP scaffold that recruits other members of DDR pathway, indicating its pivotal role in DNA repair after DNA-damaging agents (9). Since the ability of cells to effectively execute DDR signaling is essential for restoring genomic stability and for promoting survival following DNA damage, PARP-1 is fundamentally important member in response to DNA-damaging agent and overexpression of PARP-1 is often found in many cancers and considered to contribute to progression of cancer such as BRCA-mutated ovarian and breast cancer (10–12).

Renal cell carcinoma (RCC) accounts for 90% of renal cancer and its incident rate has risen during previous decade (13). Primary treatment for localized RCC is surgical resection; however, 30% of patients still continue to develop metastatic disease after surgical resection (14,15). In metastatic cancer, RT has been used for palliation routinely for brain and other extracranial lesions with respectable response rates, but a significant proportion of RCC tumors are highly radio-resistant with conventional radiation (14,15). The mechanism

associated with IR-resistance of RCC is not fully understood yet, and deeper understanding of the responsible mechanisms would provide highly appealing targets for clinical therapy.

DOC-2/DAB2 interactive protein (DAB2IP), a potent tumor suppressor, is frequently lost in RCC (16,17). DAB2IP is known to regulate various biological process including cell survival, apoptosis, as well as epithelial-to-mesenchymal transition (EMT) through the inhibition of several pathways (18). We have further demonstrated the comprehensive inhibitory mechanisms of DAB2IP on cancer stem cell regulation (19,20). Particularly, we first demonstrated the nuclear localization of DAB2IP that can impact on gene transcription (19). In this study, we observed that loss of DAB2IP in RCC cells exhibit IR-resistance and that restoration of DAB2IP expression re-sensitizes them to IR. We further identified that DAB2IP can directly interact with PARP-1 protein and affects PARP-1 protein turnover by recruiting E3-ligases (e.g. RanBP2, TRIP12, and RNF40). Indeed, PARP-1 protein expression was inversely correlated with DAB2IP expression.

As mentioned, the biological consequences of radiation leading to cell death are influenced by the activation of DDR in target cells (2). Our results clearly show that elevated PARP-1 in RCC cells may underlie IR-resistance by accelerating DDR. In contrast, knocking-down PARP-1 expression in IR-resistant RCC cells significantly increases their response to IR. Considering PARP-1 as a druggable target, we evaluated a PARP-1 inhibitor (Olaparib) in an *in vivo* RCC xenograft model as well as a patient-derived xenograft (PDX) model in combination with RT and demonstrate a significant improvement in the therapeutic efficacy of RT. Overall, this study not only unveils a mechanism of radio-resistance in RCC but also provides a rational therapeutic strategy to re-sensitize radio-resistant RCC.

Materials and Methods

Cell culture

Human RCC cell lines 786O, 769P, and ACHN cells were obtained from ATCC (Manassas, VA) and cultured in RPMI-1640 (Life Technologies) containing 10% fetal bovine serum (FBS). Immortalized human proximal tubular cell line, HK cell, was obtained from the China Center for Type Culture Collection (Wuhan, China) and cultured in RPMI-1640 containing 10% FBS, and transformed human embryonic kidney, HEK293T cells were from ATCC and cultured in Dulbecco's modified Eagle's medium (DMEM, Life Technologies) containing 5% FBS. All these cell lines were used within 15 passages and authenticated with the short tandem repeat (STR) profiling by Genomic Core in UT Southwestern (UTSW) periodically and Mycoplasma testing was performed by MycoAlert® kit (Lonza Walkersville, Inc. Walkersville, MD) every quarterly to ensure Mycoplasma-free.

Plasmid construction and reagents

The DAB2IP expression plasmid was prepared as described previously (21), and expression plasmid for human PARP-1 was obtained from Dr. Binhua Zhou (University of Kentucky College of Medicine, KY, USA) (22). Gene knockdown was performed using pLKO.1 plasmid expressing gene-specific shRNA and purchased from the National RNAi Core Facility of Taiwan (Academia Sinica, Taipei, Taiwan). Cells were plated with 70%

confluence and transfection was carried out by using Xfect (Clontech) according to the manufacturer's instructions.

Primary antibodies used were as follows: rabbit polyclonal anti-RAD51, mouse polyclonal anti-PARP-1 and monoclonal anti-BRCA1 (Santa Cruz Biotechnology, Inc.), rabbit polyclonal anti-ubiquitine (Cell signaling), anti-phospho- γ -H2AX (Ser139) (Millipore), mouse monoclonal anti-Flag and anti-actin (Sigma-Aldrich), and mouse monoclonal anti-Ku70 and 80 were home-made antibodies.

Irradiation

For *in vitro* experiment, cells were irradiated in ambient air using a JL Shepherd Mark 1–68 ^{137}Cs irradiator at a dose rate of 3.47 Gy/min (23). For *in vivo* irradiation, mice were anesthetized and subcutaneous tumors were focally irradiated using XRad 320 (Precision X-Ray, 250 kV/s, 15 mA, 20.8 Gy/min using the reference 50 mm collimator).

Clonal survival assay

Exponentially growing cells were trypsinized and counted. Cells were diluted serially to appropriate concentrations and plated onto 60-mm dish for 4 hrs. Then, cells in triplicates were treated with increasing doses of IR (0, 2, 4, 6, and 8 Gy). After 6 days of incubation, the colonies were fixed and stained with 4% formaldehyde in PBS containing 0.05% crystal violet. Colonies containing more than 50 cells were counted. Surviving fraction was calculated as $(\text{mean colony counts})/[(\text{cells inoculated for irradiation}) \times (\text{plating efficiency})]$, in which plating efficiency was defined as $(\text{mean colony counts})/(\text{cells inoculated for control})$. The data are presented as the mean \pm SEM of at least three independent experiments. The curve $S = e - (\alpha D + \beta D^2)$ was fitted to the experimental data using a least square fit algorithm using the program Sigma Plot 11.0 (Systat Software).

Double-strand break repair assay

A double-strand break (DSB) repair assay was done by counting phospho- γ H2AX foci after radiation. Cells seeded on glass coverslip were allowed to attach, and were exposed to a total dose of 2 Gy radiation. Cells were fixed with 4% paraformaldehyde and permeabilized with 0.5% Triton X-100 for 20 mins at room temperature. Then the samples were blocked with 5% bovine serum albumin and 1% normal goat serum for 1 hr. Then, cells were incubated with primary antibody, anti-phospho-Histone γ H2AX (Ser139; 1:2,000) overnight at 4°C. Samples were washed three times for 5 mins each in PBS, and then incubated with Alexa Fluor 488-conjugated secondary antibody for 1 hr. Nuclei were counterstained with DAPI and stained cells were analyzed under a fluorescence microscope (BZ-X710, Keyence).

Mass spectrometry

HEK293T cells transfected with flag-tagged DAB2IP were lysed using NE-PER™ Nuclear and Cytoplasmic Extraction Reagents (Thermo Fisher Scientific) and nuclear fraction was immunoprecipitated with anti-flag antibody. The protein complex mixtures were run into the SDS-PAGE gel and stained with Coomassie-Blue. Identification of proteins in bands cut from Coomassie-stained gel was performed by Orbitrap Elite mass-spectrometry platforms (Thermo Fisher Scientific), using short reverse-phase LC-MS/MS methods. Proteins were

identified from samples using our in-house data analysis pipeline (CPFP) of proteomics core at The University of Texas Southwestern Medical Center at Dallas.

Immunoprecipitation (IP) and Western blot

The immunocomplexes were precipitated with Dynabeads Protein G (Life Technologies) and subjected to Western blot analysis. For Western blot analysis, cells were lysed and subjected to electrophoresis on 4–12% Bolt gels (Life Technologies). Separated proteins were electroblotted onto nitrocellulose membranes, and membranes were incubated with 5% nonfat dry milk (w/v) for 1 hr and then washed in PBS containing 0.1% Tween 20. Membranes were then incubated with primary antibody, and antibody binding was detected using the appropriate secondary antibody coupled with horseradish peroxidase.

Immunohistochemistry (IHC)

Formalin-fixed, paraffin-embedded sections were de-paraffinized, rehydrated and subjected to heat-induced antigens retrieval (Citrate buffer, pH 6.0). Sections were blocked with goat serum, and incubated with appropriate primary antibody and developed with 3, 3'-diaminobenzidine chromogen followed by counterstaining with hematoxylin and eosin.

***In vivo* Ubiquitination assay**

Cells were transfected with pcDNA3.1 His-Ubiquitin and flag-DAB2IP. Approximately 36 hrs after transfection, cells were treated with 10 μ M MG132 for 6 hrs. Then, cells were harvested and the input fraction was prepared using RIPA buffer. His-tagged protein was pulled down using Dynabead® His-Tag Isolation & Pulldown (Life Technologies) according to manufacturer's instruction. The eluted samples were collected and both of the input and pull-down fraction were subjected to SDS-PAGE and Western blot analyses.

RCC xenograft, Patient-derived xenograft (PDX) models, and radiation treatment

All animal work was approved by the Institutional Animal Care and Use Committee. ACHN (3×10^6 cells/site) cells mixed with 50% Matrigel (BD Biosciences) in 0.1 ml were injected subcutaneously as well. Animals were randomly divided into four groups including untreated control, radiation alone (2 Gy), Olaparib alone (15 mg/kg), and combination treatment of radiation and Olaparib. When tumors developed to a measurable size, mice were treated with a total dose of 2 Gy using the XRad 320 (Precision X-Ray). Then, Olaparib was given orally every day for 2 weeks. Tumor volume (cubic millimeters) was measured and calculated by using the ellipsoid formula ($\pi/6 \times \text{length} \times \text{width} \times \text{depth}$).

For PDX model, frozen RCC-PDX tissue samples (20–30 mm³) from UT Southwestern Kidney Cancer and SPORE Program were implanted subcutaneously in the right posterior flanks of six-weeks-old male NOD/SCID mice (24). When tumors reached 150–200 mm³, tumor-bearing mice were randomized, anesthetized with isoflurane, and subjected to a single fraction of x-rays. Animal body weights and tumor volumes were measured twice weekly until tumor volume reached a maximum size (2000 mm³) or up to 120 days after radiation treatment. X-rays were delivered to tumor area using a 10 mm diameter collimator attached to the Xrad-320 small animal irradiator to minimized radiation exposure to the rest animal body.

Statistical analysis

All error bars in graphical data represent mean \pm SD. Student's two-tailed t-test was used for the determination of statistical relevance between groups, and $p < 0.01$ was considered statistically significant. All statistical analyses were performed with GraphPad Prism software.

Results

Decreased DAB2IP expression enhances IR-resistance in RCC

DAB2IP is a tumor-suppressor protein capable of modulating the cytoplasmic steps of various oncogenic pathways (18). In RCC, we have found that expression of DAB2IP is lost in high-grade tumors from different subtypes of RCC which is correlated with poor survival and resistance to therapy. Also, loss of DAB2IP can promote stem cell phenotypes in RCC cells (20). Thus, we further investigated whether decreased DAB2IP expression enhanced radio-resistance in RCC. Indeed, DAB2IP-negative RCC cell lines such as ACHN and 769P were more resistant to IR than their counterparts with ectopic expression of a DAB2IP cDNA; the clonal survival results indicated that DAB2IP-positive cells (D) were significantly sensitive to IR compared with those transfected with vector control (Neo) (Fig. 1A). For example, the survival fraction at 2 Gy (SF_2) for ACHN and 769P was reduced from 0.50 ± 0.005 and 0.47 ± 0.019 to 0.34 ± 0.027 and 0.33 ± 0.009 , respectively.

At the genomic level, IR can elicit both single- and double-strand DNA breaks that evoke a multifaceted DDR. Therefore, enhanced DNA repair is a mechanism whereby cells may become resistant to IR (2). An early step in DSB repair involves the rapid phosphorylation of γ H2AX at damaged sites (5,25). To measure the induction and repair of IR-induced DSBs, cells exposed to a total dose of 2 Gy were collected at the indicated times and subjected to immunofluorescence staining for phospho- γ H2AX. DSB repair kinetics can be determined by counting the phospho- γ H2AX remaining foci over time. The results showed that the rate of DSB repair was significantly increased in DAB2IP-negative cells compared with DAB2IP-positive cells (Fig. 1B). The initial expression levels of phospho- γ H2AX remaining foci were not different in DAB2IP-negative and -positive cell line. Rapid induction of DNA damage by IR was detected within 0.5 hr in all of the cell lines similarly, but more than 90% repair was completed at 8 hrs following IR in DAB2IP-negative (i.e., Neo) cells, whereas DAB2IP-positive cells still retained nearly 50% of foci even after 24 hrs. These results suggest that loss of DAB2IP in RCC enhances IR-resistance by accelerating DSB repair kinetics.

DAB2IP regulates PARP-1 protein expression through protein-protein interactions

In addition to GTPase activating protein activity, several studies have demonstrated that DAB2IP can function as a scaffold protein to interact with different enzymes or transcriptional factor involved in epigenetic regulation (19,20). Knowing the nuclear localization of DAB2IP, we decided to explore whether DAB2IP can associate with DDR machinery. Nuclear proteins were immunoprecipitated with DAB2IP antibody and subjected to mass-spectrometry; 538 protein candidates were identified (spectral counts > 3 , ratio against IgG > 2). We further analyzed these candidate proteins based on the highly

interconnected networks using Reactome (26). These proteins were involved in various biological processes including metabolism, ubiquitination, and cell cycle. Noticeably, several proteins involved in DNA repair were ranked highly in gene ontology (GO) enrichment analyses (Fig. 2A). Among them, particularly, PARP-1 was consistently and strongly associated with endogenous DAB2IP in several RCC cell lines determined by reciprocal IP (Fig. 2B). PARP-1 is a ubiquitous enzyme that transfers ADP-ribose units from donor β -NAD onto various substrate proteins (7), and commonly involved in many cellular functions such as transcriptional modulation or DDR which can facilitate repair of radiation-induced DNA breaks (8). Also, DAB2IP status does not affect the expression of key repair factors in NHEJ (Ku70, Ku80) and HR (RAD51, BRCA1) in ACHN and 769P cells (Fig.S1A). Thus, we further investigated the impact of DAB2IP on PARP-1 and observed an inverse correlation between DAB2IP and PARP-1 protein expression (Fig. 2C). PARP-1 protein expression was dramatically increased after knocking down endogenous DAB2IP in HK and 786O cells, whereas an ectopic expression of DAB2IP in 769P or 786O KD cells could suppress the expression PARP-1 protein. Consistently, the enzymatic activity of PARP-1 determined by *in vitro* assay was significantly reduced in cells with increased DAB2IP (Fig. 2D).

Importantly, in addition to *in vitro* models, we also discovered that PARP-1 protein was highly elevated in kidney tissues derived from DAB2IP-knockout mice (KO) compared with that from wild-type mice (Fig. 2E and 2F). In contrast to the significant suppression of PARP-1 protein levels by DAB2IP, PARP-1 mRNA expression levels remained unchanged in RCC cell lines or specimens (Fig. S1B and C), suggesting that DAB2IP regulates PARP-1 protein expression in post-transcription level. As we had observed that both DAB2IP and PARP-1 can be found together in a complex on immunoprecipitation experiments, we conjecture whether this interaction may regulate PARP-1 levels.

DAB2IP decreases PARP-1 protein stability

To determine the impact of DAB2IP on PARP-1 protein expression, we measured the half-life of PARP-1 reflecting its protein stability. We found that PARP-1 half-life in DAB2IP-negative cells was much longer than that in DAB2IP-positive cells, indicating that DAB2IP is involved in PARP-1 protein turnover (Fig. 3A). Indeed, the accumulation of ubiquitinated PARP-1 protein was significantly increased in DAB2IP-positive cells while the total PARP-1 was reduced (Fig. 3B). Furthermore, treatment of proteasome inhibitor (MG132) could rescue the expression of PARP-1 protein as well as enzymatic activity even in DAB2IP-positive cells (Fig. 3C and D). These data indicate that PARP-1 protein turnover requires DAB2IP and involves the ubiquitin-proteasome system (UPS).

Regulation of PARP-1 by DAB2IP is mediated by ubiquitin-proteasome system (UPS)

Next, we performed an *in vivo* ubiquitination assay to further confirm the impact of DAB2IP on regulating PARP-1 protein turnover through the UPS. As shown in Fig. 4A, incremental DAB2IP expression in HEK293T or 786O cells resulted in increased ubiquitinated PARP-1 in a dose-dependent manner suggesting that DAB2IP-mediated UPS plays an important role in regulating PARP-1 protein expression post-translationally. Although, protein ubiquitination through UPS is known to play a critical role in regulating many biological

processes such as cell cycle progression, DNA repair, apoptosis (27), how PARP-1 is ubiquitinated is not fully characterized. During UPS protein degradation, E3-ligases carry out the final step that catalyzes transfer of ubiquitin from an E2 enzyme to form a covalent bond with a substrate lysine (28). The E3-ligases therefore determine the substrate specificity, which reflects the existence of numerous different E3-ligases compared with few E1 and E2-enzymes (29). To identify the candidate E3-ligases recruited by DAB2IP during PARP-1 degradation, we performed immunoprecipitation followed by Mass Spectrometry (IP-MS) from MG132 treated cells. Briefly, HEK293T cell transfected with DAB2IP expressing plasmid was treated with MG132 for 6 hrs, then cell lysates were immunoprecipitated with PARP-1 or DAB2IP antibody and subjected to MS. Based on IP-MS data, we found three E3-ligases (i.e., RanBP2, TRIP12, and RNF40) consistently associated with both PARP-1 and DAB2IP as potential candidates (Fig. S2A). We further performed IP to validate the interaction both DAB2IP and PARP-1 with the 3 different E3-ligases in DAB2IP-negative (293T-Neo) vs. DAB2IP-positive (293T-D) cells; the protein-protein interaction was clearly detected in 293T-D cells but not in 293T-Neo cells indicating that the presence of DAB2IP can accelerate these E3-ligases to degrade PARP-1 protein (Fig. 4B).

To examine the functional role of individual E3-ligases on PARP-1 degradation, DAB2IP-positive RCC cells were transfected with shRNA specifically targeting each E3-ligase. As shown in Figure 4C, knockdown of the individual E3-ligases remarkably decreased ubiquitinated PARP-1 levels and increased PARP-1 protein expression even in the presence of DAB2IP. These results indicate RanBP2, TRIP12, and RNF40 are critical mediators in PARP-1 protein degradation system, but DAB2IP is required to finish UPS. In contrast, knockdown of the E3 ligase pVHL that is not associated with DAB2IP, did not affect PARP-1 protein expression.

To further confirm our findings, TCGA database was analyzed for possible clinical relevance of these 3 E3-ligase in RCC, and RanBP2 was found to be significantly downregulated in tumor tissues compared with the adjacent normal tissues and this correlated with disease progression (Fig. S2B) as well as overall survival of RCC patients (Fig. S2C). Consistently, knocking down of RanBP2 mRNA expression restored PARP-1 enzyme activity in DAB2IP-positive cells suggesting the critical functional role of RanBP2 in degrading PARP-1 in RCC (Fig. 4D). Furthermore, the stable RanBP2 knockdown RCC cells (Fig.4E) acquired radio-resistance compared with parental DAB2IP-positive cells (Fig. 4F). Altogether, this is a novel mechanism of regulation of PARP-1 protein degradation by specific E3-ligase mediated by a scaffold function of DAB2IP.

Targeting PARP-1 increases the efficacy of radiotherapy in RCC

We next evaluated the rescue effect of PARP-1 on radio-resistance. As shown in Figure 5A and B, constitutive overexpression of PARP-1 induced radio-resistance in DAB2IP-positive cells whereas knockdown of PARP-1 increased IR-sensitivity in DAB2IP-negative cells.

The role of PARP-1 in radio-resistance of RCC highlights the potential application of PARP-1 inhibitors on RT in RCC tumors. The efficacy of either a single agent PARP-1 inhibitor or in combination with other cytotoxic drugs has been demonstrated in many types

of cancer (30,31) but not in RCC. Olaparib (AZD2281) is a small molecule PARP-1/2 inhibitor, currently under evaluation in many clinical trials of breast, uterine, colorectal and ovarian cancers already FDA-approved for some indications (32,33). To explore the effect of Olaparib on radio-resistant RCC cells (i.e., DAB2IP-negative cells), cells were treated with Olaparib for 6 hrs prior to IR. The results showed that Olaparib could sensitize those resistant cells to IR in a dose-dependent manner (Fig. 5C). Therefore, we found that PARP-1 is responsible for radio-resistance of RCC cells, and could be a potential target to enhance the efficacy of RT in RCC treatment.

PARP-1 inhibitor enhances *in vivo* IR effect on RCC tumors

To further demonstrate the effect of PARP-1 inhibitor as a radio-sensitizer in RCC tumor, we employed a mouse xenograft model carrying ACHN tumors. Radiation was administered as single treatment of 2 Gy at Day 0, and Olaparib was given orally daily for two weeks. Treatment with low dose of Olaparib (15 mg/kg, oral gavage daily for 2 weeks) transiently suppressed the tumor growth in the first week after starting treatment ($p < 0.05$ at Day 7), but tumors re-grew shortly thereafter ($p = 0.128$ and 0.185 at Day 10 and Day 14, respectively) (Fig. 6A). Combination therapy, however, shows a robust inhibition of tumor growth compared with tumors treated with IR alone or Olaparib alone ($p < 0.05$ at 1 week post-treatment) without body weight changes (Fig. 6A and Fig. S3A). In comparison to control, the combination treatment showed a remarkable therapeutic efficacy (Fig. 6A and S3A).

Having confirmed the better efficacy of combination therapy, the strategy was extended to the evaluation of PDX models (XP490 and XP334). We selected two PDX models with different levels of DAB2IP and PARP-1, XP490, which had higher DAB2IP levels but lower PARP-1 and XP334 (Fig. 6B). Notably, XP490 was very sensitive to IR (Fig. 6C). In contrast, XP334 showed more resistant to either IR or Olaparib alone, but Olaparib was able to sensitize XP334 cells to IR (Fig. 6D), when used in combination. From genetic profiling of these PDX models, it seems that the IR resistance is independent of the status of VHL, BAP1, and PBRM1 (Fig. S3B). On the other hand, XP334 PDX model appeared to be more resistant to IR compare with XP374 which exhibited higher DAB2IP (Fig. S3D). These data suggest that DAB2IP levels in company with PARP-1 could provide the prediction of the IR sensitivity. Taken together, we conclude that the down regulation of DAB2IP underlies IR resistance in RCC cells.

Discussion

PARP-1 is an ADP-ribosylating enzyme that is activated upon binding to DNA breakpoint induced by IR (7). The critical role of PARP-1 in DNA repair is reflected by its frequent upregulation in cancer cells such as melanomas and breast cancer. Therefore, elevated PARP-1 expression is often considered to be a prognostic feature associated with poor survival rate of cancer patients (10,34,35). However, in RCC, the regulation of PARP-1 and its role are not well characterized. In this study, we unveiled a unique mechanism of regulating PARP-1 protein stability by the DAB2IP-E3 ligase complex. Over the past decades, several studies have demonstrated that posttranslational modifications of PARP-1, including ADP-ribosylation, phosphorylation, and acetylation have differential impact on its

downstream functions (7,9,36) but little is known about PARP-1 ubiquitylation. In an early study, Wang *et al.* suggested that K48 is the major site for PARP-1 polyubiquitination in mouse fibroblast cells leading to protein degradation, and assumed that the polyubiquitination site might be away from the catalytic domain or the automodification site of PARP-1, because NAD⁺ inhibited PARP-1 ubiquitination (37). Another study in heat shocked HeLa cells indicated that ubiquitinated PARP-1 was bound by E3-ligase RNF4, which led to the clearance and recycling of PARP-1 from the promoter region of target genes (38). In this study, we identify several specific E3-ligases such as RanBP2, TRIP12, and RNF40, responsible for PARP-1 polyubiquitination. More importantly, tumor suppressor DAB2IP is able to facilitate PARP-1 polyubiquitination, which subsequently leads to the reduction of PARP-1 protein levels. A significant clinical correlation of RanBP2 expression is found with overall survival of RCC patients, supporting the notion that post-translation modification of PARP-1 plays a critical role in RCC development. The elevated PARP-1 expression facilitates the rapid DSB repair that underlies the radio-resistance of many malignant cells. Thus, PARP-1 inhibitors (PARPi) have recently been evaluated as a sensitizer for RT in different cancer types; Olaparib (AZD2281) is currently being examined for breast or ovarian cancers with *BRCA1/2* mutation (39). Initial trials have demonstrated significant efficacy for both cancer patients who harbor germ line *BRCA1/2* mutation; suggesting *BRCA1/2* as a selective biomarker for this regimen (40,41). In addition to breast and ovarian cancer, *BRCA1/2* mutations have also increased life-time risk of pancreas, colon, and prostate cancers; Olaparib treatment showed better clinical benefit to those *BRCA1/2* mutation-associated patients (33,42–44). In contrast, *BRCA1/2* mutation, was not commonly associated with RCC patients (45). However, increasing studies indicate a potential therapeutic role for PARPi in broader subgroup of solid tumors that have homologous recombination dysfunction (HRD) (46,47). Patients with HRD, but not *BRCA1/2* mutation also showed ‘BRCA-like’ behavior, such as susceptibility to DNA damage agents (11,48). For example, loss of function of PTEN has been shown to yield BRCA-like behavior and increased PARPi susceptibility was shown in tumors harboring PTEN mutation or haploinsufficiency, suggesting PTEN-loss also could be a potential biomarker for predicting PARPi responsiveness (49,50). Given that efficacy of PARPi in other solid tumors not harboring *BRCA1/2* mutations, suggested that PARPi potentially have a broader application in treatment of cancer patients than was previously envisioned, possibly through different mechanisms of action. Indeed, our study demonstrated new evidence for PARPi susceptibility in RCC. The outcome of this study further suggests that either DAB2IP or RanBP2 should be further evaluated as selective biomarker(s) for targeted RT in RCC patients. Our understanding of the molecular mechanism underlying radio-resistant RCC unveils a potent target- PARP-1 and the effect of Olaparib on enhancing the efficacy of RT from both *in vitro* and *in vivo* models provides a strong rationale to develop a clinical trial of combining PARPi with IR to overcome radio-resistant RCC tumors that have lost DAB2IP expression.

Supplementary Material

Refer to Web version on PubMed Central for supplementary material.

Acknowledgment

We thank Dr. Samarпита Sengupta for editorial assistance. This study was supported in part by the National Research Foundation of Korea (NRF-2018R1D1A1B07040751 to EJY, NRF-2018M3C7A1024152 to STB), BK21 Plus funded by Ministry of Education of Korea (10Z20130012243 to EJY), National Cancer Institute SPORE (P50CA196516 to JB), the Ministry of Science and Technology in Taiwan (MOST103-2911-I-005-507 to HL) and Cancer Prevention Research Institute of Texas (RP160268 to BPC).

References

1. Mladenov E, Magin S, Soni A, Iliakis G. DNA double-strand break repair as determinant of cellular radiosensitivity to killing and target in radiation therapy. *Frontiers in oncology* 2013;3:113. [PubMed: 23675572]
2. Willers H, Dahm-Daphi J, Powell SN. Repair of radiation damage to DNA. *British journal of cancer* 2004;90:1297–301. [PubMed: 15054444]
3. Hoeijmakers JH. DNA damage, aging, and cancer. *The New England journal of medicine* 2009;361:1475–85. [PubMed: 19812404]
4. Jackson SP. The DNA-damage response: new molecular insights and new approaches to cancer therapy. *Biochem Soc Trans* 2009;37:483–94. [PubMed: 19442242]
5. Rogakou EP, Boon C, Redon C, Bonner WM. Megabase chromatin domains involved in DNA double-strand breaks in vivo. *J Cell Biol* 1999;146:905–16. [PubMed: 10477747]
6. Taverna SD, Li H, Ruthenburg AJ, Allis CD, Patel DJ. How chromatin-binding modules interpret histone modifications: lessons from professional pocket pickers. *Nature structural & molecular biology* 2007;14:1025–40.
7. Kim MY, Zhang T, Kraus WL. Poly(ADP-ribosyl)ation by PARP-1: ‘PAR-laying’ NAD⁺ into a nuclear signal. *Genes & development* 2005;19:1951–67. [PubMed: 16140981]
8. Chalmers A, Johnston P, Woodcock M, Joiner M, Marples B. PARP-1, PARP-2, and the cellular response to low doses of ionizing radiation. *International journal of radiation oncology, biology, physics* 2004;58:410–9.
9. Krishnakumar R, Kraus WL. PARP-1 regulates chromatin structure and transcription through a KDM5B-dependent pathway. *Molecular cell* 2010;39:736–49. [PubMed: 20832725]
10. Rojo F, Garcia-Parra J, Zazo S, Tusquets I, Ferrer-Lozano J, Menendez S, et al. Nuclear PARP-1 protein overexpression is associated with poor overall survival in early breast cancer. *Annals of oncology : official journal of the European Society for Medical Oncology* 2012;23:1156–64. [PubMed: 21908496]
11. Safra T, Borgato L, Nicoletto MO, Rolnitzky L, Pelles-Avraham S, Geva R, et al. BRCA mutation status and determinant of outcome in women with recurrent epithelial ovarian cancer treated with pegylated liposomal doxorubicin. *Molecular cancer therapeutics* 2011;10:2000–7. [PubMed: 21835933]
12. Dziaman T, Ludwiczak H, Ciesla JM, Banaszkiwicz Z, Winczura A, Chmielarczyk M, et al. PARP-1 expression is increased in colon adenoma and carcinoma and correlates with OGG1. *PLoS One* 2014;9:e115558. [PubMed: 25526641]
13. Volpe A, Patard JJ. Prognostic factors in renal cell carcinoma. *World J Urol* 2010;28:319–27. [PubMed: 20364259]
14. De Meerleer G, Khoo V, Escudier B, Joniau S, Bossi A, Ost P, et al. Radiotherapy for renal-cell carcinoma. *The Lancet Oncology* 2014;15:e170–7. [PubMed: 24694640]
15. Blanco AI, Teh BS, Amato RJ. Role of radiation therapy in the management of renal cell cancer. *Cancers* 2011;3:4010–23. [PubMed: 24213122]
16. Zhou J, Luo J, Wu K, Yun EJ, Kapur P, Pong RC, et al. Loss of DAB2IP in RCC cells enhances their growth and resistance to mTOR-targeted therapies. *Oncogene* 2016;35:4663–74. [PubMed: 26876207]
17. Wang ZR, Wei JH, Zhou JC, Haddad A, Zhao LY, Kapur P, et al. Validation of DAB2IP methylation and its relative significance in predicting outcome in renal cell carcinoma. *Oncotarget* 2016;7:31508–19. [PubMed: 27129174]

18. Liu L, Xu C, Hsieh JT, Gong J, Xie D. DAB2IP in cancer. *Oncotarget* 2016;7:3766–76. [PubMed: 26658103]
19. Yun EJ, Baek ST, Xie D, Tseng SF, Dobin T, Hernandez E, et al. DAB2IP regulates cancer stem cell phenotypes through modulating stem cell factor receptor and ZEB1. *Oncogene* 2015;34:2741–52. [PubMed: 25043300]
20. Yun EJ, Zhou J, Lin CJ, Xu S, Santoyo J, Hernandez E, et al. The network of DAB2IP-miR-138 in regulating drug resistance of renal cell carcinoma associated with stem-like phenotypes. *Oncotarget* 2017;8:66975–86. [PubMed: 28978010]
21. Zhang R, He X, Liu W, Lu M, Hsieh JT, Min W. AIP1 mediates TNF-alpha-induced ASK1 activation by facilitating dissociation of ASK1 from its inhibitor 14-3-3. *The Journal of clinical investigation* 2003;111:1933–43. [PubMed: 12813029]
22. Lin Y, Kang T, Zhou BP. Doxorubicin enhances Snail/LSD1-mediated PTEN suppression in a PARP1-dependent manner. *Cell cycle* 2014;13:1708–16. [PubMed: 24675890]
23. Kodym E, Kodym R, Reis AE, Habib AA, Story MD, Saha D. The small-molecule CDK inhibitor, SNS-032, enhances cellular radiosensitivity in quiescent and hypoxic non-small cell lung cancer cells. *Lung cancer* 2009;66:37–47. [PubMed: 19193471]
24. Pavia-Jimenez A, Tcheuyap VT, Brugarolas J. Establishing a human renal cell carcinoma tumorgraft platform for preclinical drug testing. *Nat Protoc* 2014;9:1848–59. [PubMed: 25010905]
25. Asaithamby A, Chen DJ. Cellular responses to DNA double-strand breaks after low-dose gamma-irradiation. *Nucleic acids research* 2009;37:3912–23. [PubMed: 19401436]
26. Fabregat A, Sidiropoulos K, Garapati P, Gillespie M, Hausmann K, Haw R, et al. The Reactome pathway Knowledgebase. *Nucleic acids research* 2016;44:D481–7. [PubMed: 26656494]
27. Pickart CM. Mechanisms underlying ubiquitination. *Annual review of biochemistry* 2001;70:503–33.
28. Berndsen CE, Wolberger C. New insights into ubiquitin E3 ligase mechanism. *Nature structural & molecular biology* 2014;21:301–7.
29. Dikic I, Robertson M. Ubiquitin ligases and beyond. *BMC biology* 2012;10:22. [PubMed: 22420755]
30. Bolderson E, Richard DJ, Zhou BB, Khanna KK. Recent advances in cancer therapy targeting proteins involved in DNA double-strand break repair. *Clinical cancer research : an official journal of the American Association for Cancer Research* 2009;15:6314–20.
31. Rowe BP, Glazer PM. Emergence of rationally designed therapeutic strategies for breast cancer targeting DNA repair mechanisms. *Breast cancer research : BCR* 2010;12:203. [PubMed: 20459590]
32. Rouleau M, Patel A, Hendzel MJ, Kaufmann SH, Poirier GG. PARP inhibition: PARP1 and beyond. *Nature reviews Cancer* 2010;10:293–301. [PubMed: 20200537]
33. Fong PC, Boss DS, Yap TA, Tutt A, Wu P, Mergui-Roelvink M, et al. Inhibition of poly(ADP-ribose) polymerase in tumors from BRCA mutation carriers. *The New England journal of medicine* 2009;361:123–34. [PubMed: 19553641]
34. Galia A, Calogero AE, Condorelli R, Frassetta F, La Corte A, Ridolfo F, et al. PARP-1 protein expression in glioblastoma multiforme. *European journal of histochemistry : EJH* 2012;56:e9. [PubMed: 22472897]
35. Csete B, Lengyel Z, Kadar Z, Battyani Z. Poly(adenosine diphosphate-ribose) polymerase-1 expression in cutaneous malignant melanomas as a new molecular marker of aggressive tumor. *Pathology oncology research : POR* 2009;15:47–53. [PubMed: 18752052]
36. Luo X, Kraus WL. On PAR with PARP: cellular stress signaling through poly(ADP-ribose) and PARP-1. *Genes & development* 2012;26:417–32. [PubMed: 22391446]
37. Wang T, Simbulan-Rosenthal CM, Smulson ME, Chock PB, Yang DC. Polyubiquitylation of PARP-1 through ubiquitin K48 is modulated by activated DNA, NAD+, and dipeptides. *Journal of cellular biochemistry* 2008;104:318–28. [PubMed: 18041763]
38. Martin N, Schwamborn K, Schreiber V, Werner A, Guillier C, Zhang XD, et al. PARP-1 transcriptional activity is regulated by sumoylation upon heat shock. *The EMBO journal* 2009;28:3534–48. [PubMed: 19779455]

39. Ledermann J, Harter P, Gourley C, Friedlander M, Vergote I, Rustin G, et al. Olaparib maintenance therapy in patients with platinum-sensitive relapsed serous ovarian cancer: a preplanned retrospective analysis of outcomes by BRCA status in a randomised phase 2 trial. *The Lancet Oncology* 2014;15:852–61. [PubMed: 24882434]
40. Audeh MW, Carmichael J, Penson RT, Friedlander M, Powell B, Bell-McGuinn KM, et al. Oral poly(ADP-ribose) polymerase inhibitor olaparib in patients with BRCA1 or BRCA2 mutations and recurrent ovarian cancer: a proof-of-concept trial. *Lancet* 2010;376:245–51. [PubMed: 20609468]
41. Tutt A, Robson M, Garber JE, Domchek SM, Audeh MW, Weitzel JN, et al. Oral poly(ADP-ribose) polymerase inhibitor olaparib in patients with BRCA1 or BRCA2 mutations and advanced breast cancer: a proof-of-concept trial. *Lancet* 2010;376:235–44. [PubMed: 20609467]
42. Risch HA, McLaughlin JR, Cole DE, Rosen B, Bradley L, Fan I, et al. Population BRCA1 and BRCA2 mutation frequencies and cancer penetrances: a kin-cohort study in Ontario, Canada. *Journal of the National Cancer Institute* 2006;98:1694–706. [PubMed: 17148771]
43. Thompson D, Easton DF, Breast Cancer Linkage C. Cancer Incidence in BRCA1 mutation carriers. *Journal of the National Cancer Institute* 2002;94:1358–65. [PubMed: 12237281]
44. Brose MS, Rebbeck TR, Calzone KA, Stopfer JE, Nathanson KL, Weber BL. Cancer risk estimates for BRCA1 mutation carriers identified in a risk evaluation program. *Journal of the National Cancer Institute* 2002;94:1365–72. [PubMed: 12237282]
45. Mersch J, Jackson MA, Park M, Nebgen D, Peterson SK, Singletary C, et al. Cancers associated with BRCA1 and BRCA2 mutations other than breast and ovarian. *Cancer* 2015;121:269–75. [PubMed: 25224030]
46. Turner N, Tutt A, Ashworth A. Hallmarks of ‘BRCAness’ in sporadic cancers. *Nature reviews Cancer* 2004;4:814–9. [PubMed: 15510162]
47. Yap TA, Sandhu SK, Carden CP, de Bono JS. Poly(ADP-ribose) polymerase (PARP) inhibitors: Exploiting a synthetic lethal strategy in the clinic. *CA: a cancer journal for clinicians* 2011;61:31–49. [PubMed: 21205831]
48. Gallagher DJ, Konner JA, Bell-McGuinn KM, Bhatia J, Sabbatini P, Aghajanian CA, et al. Survival in epithelial ovarian cancer: a multivariate analysis incorporating BRCA mutation status and platinum sensitivity. *Annals of oncology : official journal of the European Society for Medical Oncology* 2011;22:1127–32. [PubMed: 21084428]
49. Fraser M, Zhao H, Luoto KR, Lundin C, Coackley C, Chan N, et al. PTEN deletion in prostate cancer cells does not associate with loss of RAD51 function: implications for radiotherapy and chemotherapy. *Clinical cancer research : an official journal of the American Association for Cancer Research* 2012;18:1015–27. [PubMed: 22114138]
50. Forster MD, Dedes KJ, Sandhu S, Frentzas S, Kristeleit R, Ashworth A, et al. Treatment with olaparib in a patient with PTEN-deficient endometrioid endometrial cancer. *Nature reviews Clinical oncology* 2011;8:302–6.

Translational relevance

Renal cell carcinoma (RCC) is by far the most lethal urologic malignancy and often resistant to ionizing radiation (IR). The mechanisms leading to IR-resistance are not fully understood. Here, we determine that loss of DAB2IP in RCC cells contribute to their radio-resistance, which is correlated with elevated PARP-1 levels that could repair DNA damage caused by radiation. We further unveil a new mechanism of DAB2IP in modulating PARP-1 protein degradation by recruiting an E3 ligase (RANBP2). Thus, targeting PARP-1 using small molecule inhibitor can sensitize resistant RCC to IR both *in vitro* and *in vivo* models. In conclusion, DAB2IP loss in RCC results in IR resistance that can be overcome with PARP-1 inhibitors.

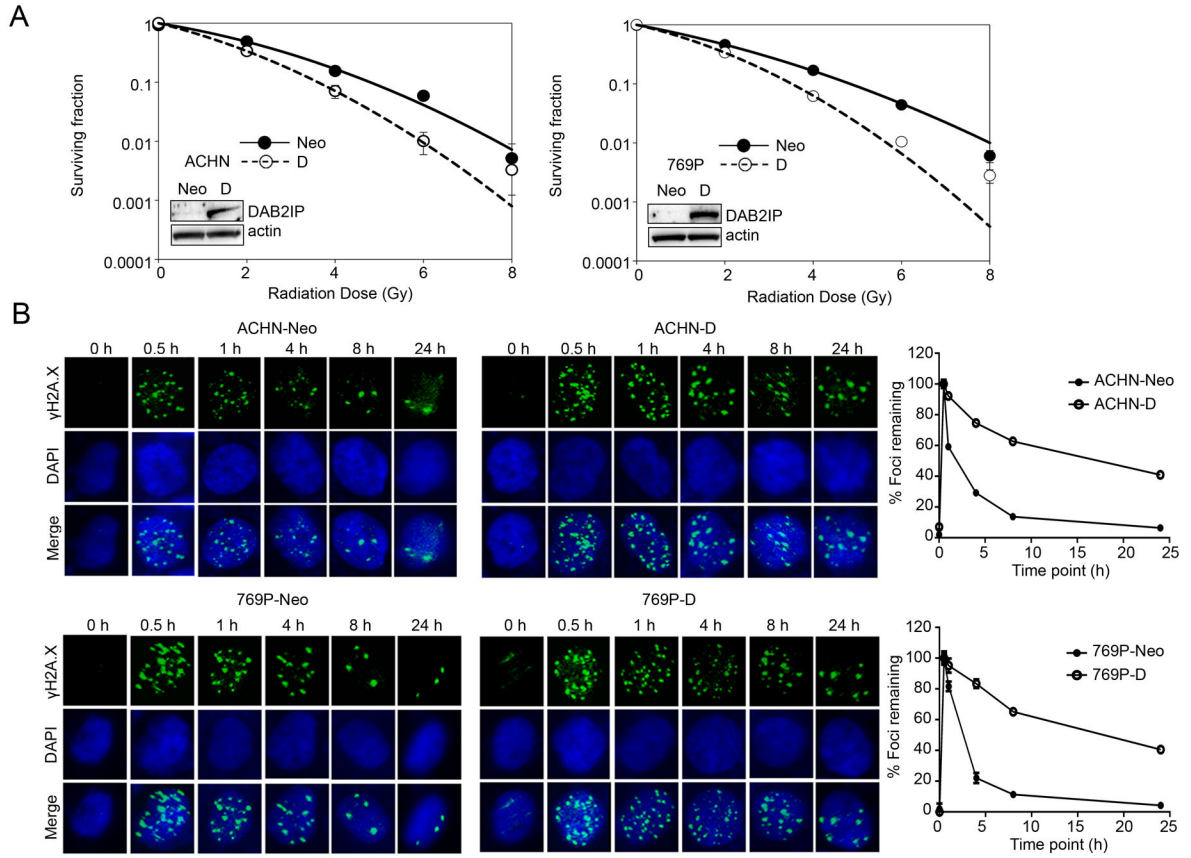


Figure 1. DAB2IP decreases radio-resistance of RCC.

(A) Cells were exposed to incremental doses of radiation. After 7 days of culture, colonies were counted and survival fractions were constructed by fitting mean values from three independent experiments to a linear quadratic model. (B) After irradiation with 2 Gy, cells were stained with phospho- γ H2AX (green) at the indicated time point to determine remaining foci formation. DNA repair kinetics of cells was obtained by plotting the percentage of remaining foci against time.

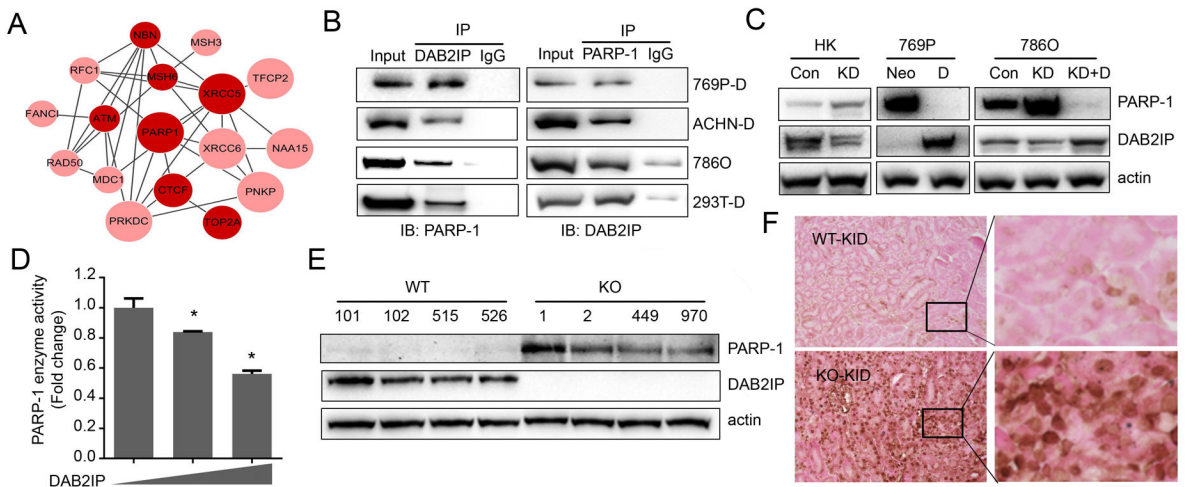


Figure 2. DAB2IP interacts with PARP-1 protein.

(A) DAB2IP interacting proteins identified via Mass-spectrometry were analyzed using Reactome and highly interconnected networks of proteins were constructed. Node size correlates with number of links, and node darkness indicates relation to cancer progression. (B) Cell lysates were extracted from various RCC cell lines, and interaction of DAB2IP with PARP-1 was validated by IP. (C) PARP-1 protein expressions were compared between DAB2IP-positive and -negative cells by Western blot analysis. (D) 293T cells were transfected with incremental dose of DAB2IP and enzymatic activity of PARP-1 was measured. (E and F) PARP-1 expression in wild-type (WT) and DAB2IP knockout (KO) mice kidney tissues were compared by Western blot (E) and IHC (F).

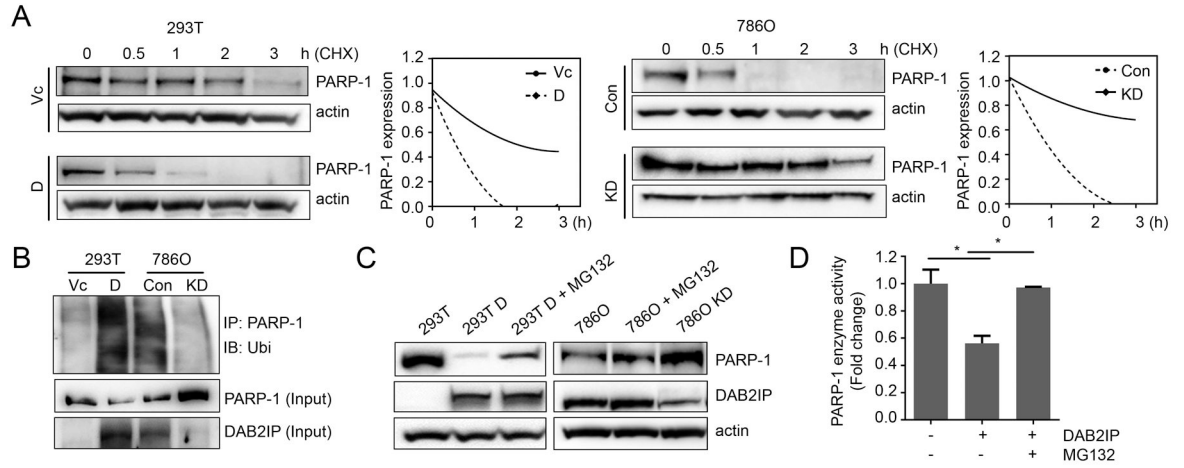


Figure 3. DAB2IP modulates the stability of PARP-1.

(A) Cells were treated with 50 $\mu\text{g/ml}$ cycloheximide (CHX) for indicated times and PARP-1 protein expression was analyzed by Western blot to determine protein half-life. (B) Cell lysates were pull down with PARP-1 antibody and blotted with ubiquitin (Ubi) antibody to compare ubiquitinated-PARP-1 expression. (C and D) Cells were treated with MG132 (10 μM , 6 hrs), and the expression levels of both PARP-1 and DAB2IP protein were determined using Western blot (C) and PARP-1 enzymatic activity was measured by ELISA assay (D).

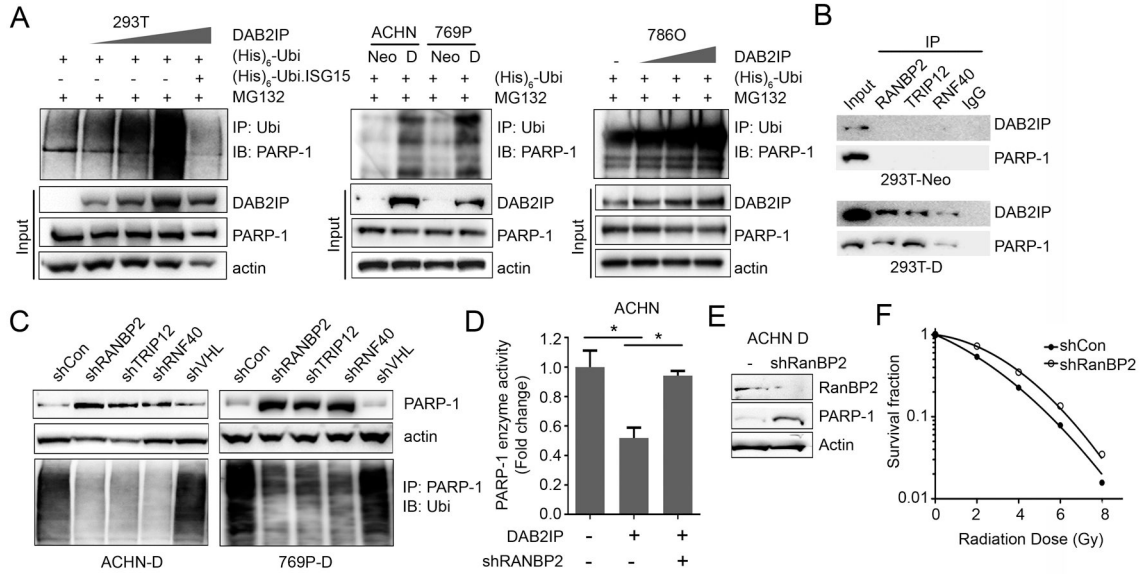


Figure 4. Regulation of PARP-1 by DAB2IP is mediated by ubiquitin-proteasome system.

(A) Cells transfected with indicated plasmids were treated with 10 μ M MG132 for 6 hrs.

Then the ubiquitinated PARP-1 was determined using *in vivo* ubiquitination assay.

Ubi.ISG15, ubiquitin-like interferon stimulated gene was used as a negative control. (B) Cell

lysates were extracted from DAB2IP-deficient or DAB2IP-overexpressing cells, and interaction of RanBP2, TRIP12, and RNF40 with DAB2IP and/or PARP-1 was validated by

IP. (C) The shRNA plasmid encoding each E3-ligase (e.g. RanBP2, TRIP12, RNF40, and

VHL) was transfected into cells expressing DAB2IP (i.e., ACHN-D and 769P-D), and PARP-1 protein expression was determined using Western blot analysis. The ubiquitinated

PARP-1 was determined by IP with PARP-1. (D) The RanBP2 expression was knock-

downed in DAB2IP-positive cells and PARP-1 enzymatic activity was compared by ELISA

assay. (E) The PARP-1 protein expression was characterized in shRanBP2 knockdown cells.

(F) Radio-resistance of shRanBP2 knockdown cells was determined by the survival fraction

of cells exposed to the incremental doses of radiation.

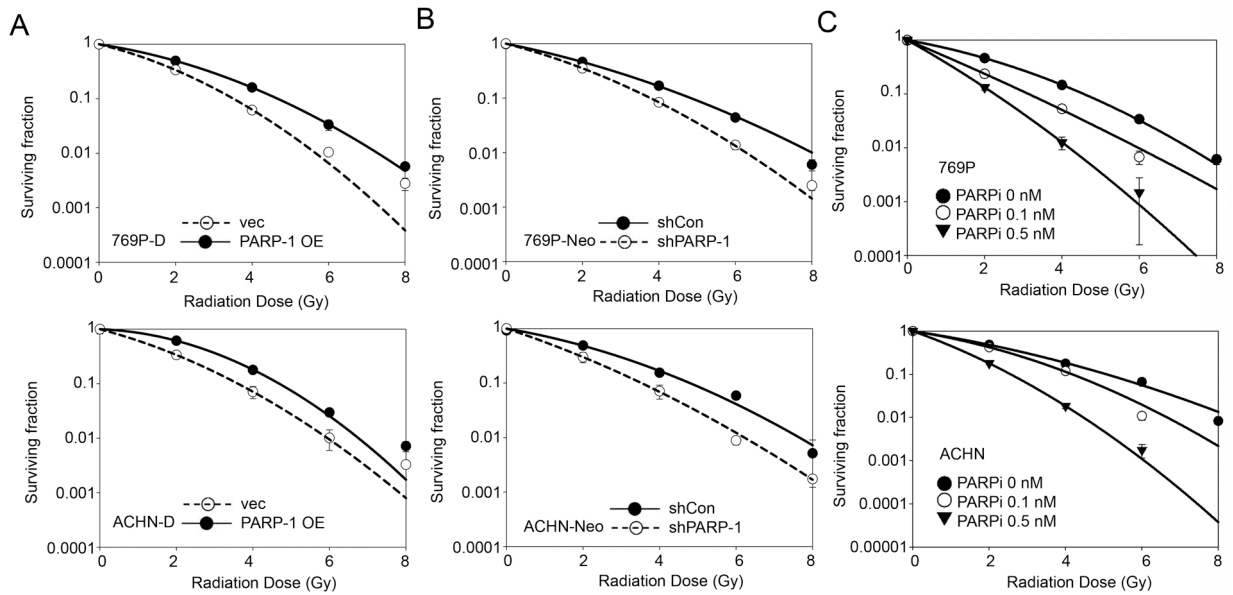


Figure 5. Targeting PARP-1 sensitizes RCC cells to IR treatment.

(A) Constitutive active PARP-1 mutant plasmid was transfected into DAB2IP-positive 769P (i.e., 769P-D) and ACHN (i.e., ACHN-D) cells, then cells were exposed to incremental doses of radiation. Cell survival fraction was analyzed 7 days after IR. (B) PARP-1 expression was knock-downed in DAB2IP-negative 769P-Neo and ACHN-Neo cells, then cells were exposed to radiation, and survival fractions were analyzed after 7 days. (C) The wild-type 769P and ACHN cells were irradiated with incremental doses and incubated with PARP-1 inhibitor (e.g. Olaparib) for 7 days. The media containing Olaparib were replenished every two days. After 7 days, colonies were counted and survival fractions were constructed by fitting mean values from three independent experiments to linear-quadratic model.

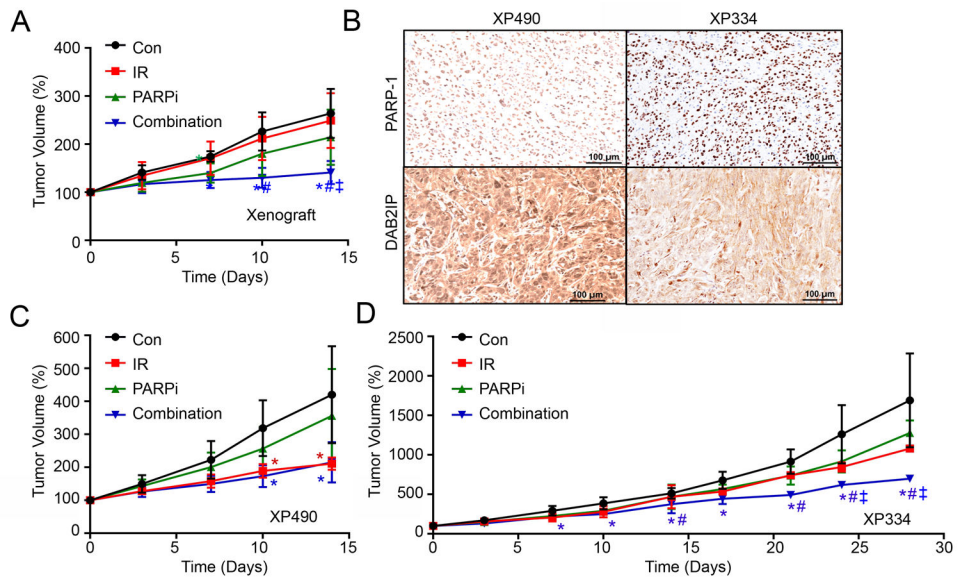


Figure 6. Targeting PARP-1 enhances the efficacy of radiotherapy *in vivo*.

(A, C and D) ACHN (3×10^6 cells/site) cells (A) as well as patient-derived xenograft XP490 (C), or XP334 (D) were subcutaneously injected into SCID mice. The mice were randomly divided into 4 groups (Con, IR, PARPi, and Combination), and each group was treated with radiation alone (2Gy, single treatment), Olaparib (15 mg/kg, oral gavage daily), or combination for 2 weeks. Tumor volumes were measured twice-a-week. Con, non-treated control; IR, irradiation only; PARPi, Olaparib treatment; Combination, irradiation + Olaparib treatment. Error bars are mean \pm S.D. Significance were indicated $p < 0.05$ by Student's *t*-Test against to Con (*), IR (#), and PARPi (‡).

(B) PAPR-1 and DAB2IP protein expression in XP490 and XP334 were compared by immunohistochemistry.